

# Quantifying Lake Athabasca (Canada) water level during the 'Little Ice Age' highstand from palaeolimnological and geophysical analyses of a transgressive barrier-beach complex

The Holocene  
20(5) 801–811  
© The Author(s) 2010  
Reprints and permission:  
sagepub.co.uk/journalsPermissions.nav  
DOI: 10.1177/0959683610362816  
<http://hol.sagepub.com>  
SAGE

John W. Johnston,<sup>1</sup> Dörte Köster,<sup>2</sup> Brent B. Wolfe,<sup>1</sup> Roland I. Hall,<sup>2</sup> Thomas W.D. Edwards,<sup>2</sup> Anthony L. Endres,<sup>2</sup> Margaret E. Martin,<sup>2</sup> Johan A. Wiklund<sup>2</sup> and Caleb Light<sup>1</sup>

## Abstract

We combine multiproxy palaeolimnological and geophysical analyses of a barrier-beach complex to estimate the water level of a sustained Lake Athabasca (Canada) highstand during the 'Little Ice Age' (LIA; 1600–1900 CE). Palaeolimnological analyses on sediment cores from the lagoon behind the barrier indicate high water levels during the LIA, controlled by subsurface hydrological connection with Lake Athabasca. Key features in the LIA stratigraphic interval are sand laminations deposited by overwash events and low C/N ratios reflecting deposition of predominantly aquatic organic matter. Ground penetrating radar profiles of the barrier reveal a depositional transgression sequence composed of waterlain landward-dipping foreset beds and horizontal topset beds, overlain by aeolian deposits. Stratigraphic relations suggest that the LIA washover deposits in the lagoon formed as the barrier was actively translating landward, and were generated by high-water events on Lake Athabasca that overtopped the barrier. This indicates Lake Athabasca rose to at least the elevation defined by the contact between the waterlain and aeolian sediments in the barrier, which is >4 m above the historical daily average from gauged records available since 1930 and likely represents storm events during the highstand. Assuming a similar relation between daily average and maximum lake level as in the historical gauge record, our findings suggest that Lake Athabasca was on average 2.3 m higher during the LIA than present day. Extrapolation of this high-water plane into the adjacent Peace-Athabasca Delta indicates that 70% of the modern landscape was frequently and perennially flooded until very recently, consistent with palaeolimnological evidence from several lakes in the delta.

## Keywords

ground-penetrating radar, Lake Athabasca, lake level, 'Little Ice Age', Peace-Athabasca Delta, transgressive barrier

## Introduction

Quantification of the marked climate-driven changes in the level of Lake Athabasca that have occurred during the past millennium (Sinnatamby *et al.*, 2010; Wolfe *et al.*, 2008) is needed to better anticipate the impact of ongoing and future climate change on the Mackenzie River system. A key episode was the 'Little Ice Age' (LIA; 1600–1900 CE; Sinnatamby *et al.*, 2010) when Lake Athabasca rose in response to increased summer river discharge, but the magnitude of water-level change is unknown. In the Laurentian Great Lakes, analysis of shoreline features has provided crucial documentation of water-level fluctuations and insight into their causes over the late Holocene (Baedke and Thompson, 2000; Johnston *et al.*, 2004, 2007; Polderman and Pryor, 2004; Thompson and Baedke, 1997). Here we utilize information contained in a transgressive barrier-beach complex on Bustard Island near the western end of Lake Athabasca, in combination with other palaeolimnological evidence and historical water-level gauge records, to provide the first estimate of water level during the lake's LIA highstand. This approach identifies a prolonged rise of ~2.3 m in average lake level during the LIA, which inundated ~70% of the present-day delta under a shallow western-extending embayment of Lake Athabasca.

## Study area

Bustard Island contains several isolated wooded areas, low-lying wetlands and two shallow ponds (Figure 1). Elevated areas of the island were mapped as an esker, composed of glaciofluvial deposits of outwash sand and gravel elongated in the direction of meltwater flow (Bednarski, 1999). Two northeast-facing embayments on the island contain components of a typical barrier-beach complex (modern beach, barrier and lagoon). Aeolian deposits cap the two barriers. The relatively narrow barrier width and morphology, which contains a single foredune ridge and several washover aprons, indicate that

<sup>1</sup>Wilfrid Laurier University, Canada

<sup>2</sup>University of Waterloo, Canada

Received 21 October 2009; revised manuscript accepted 27 December 2009

## Corresponding author:

John W. Johnston, Department of Geography and Environmental Studies, Wilfrid Laurier University, 75 University Ave. W, Waterloo, Ontario N2L 3C5, Canada  
Email: [jjohnston@wlu.ca](mailto:jjohnston@wlu.ca)

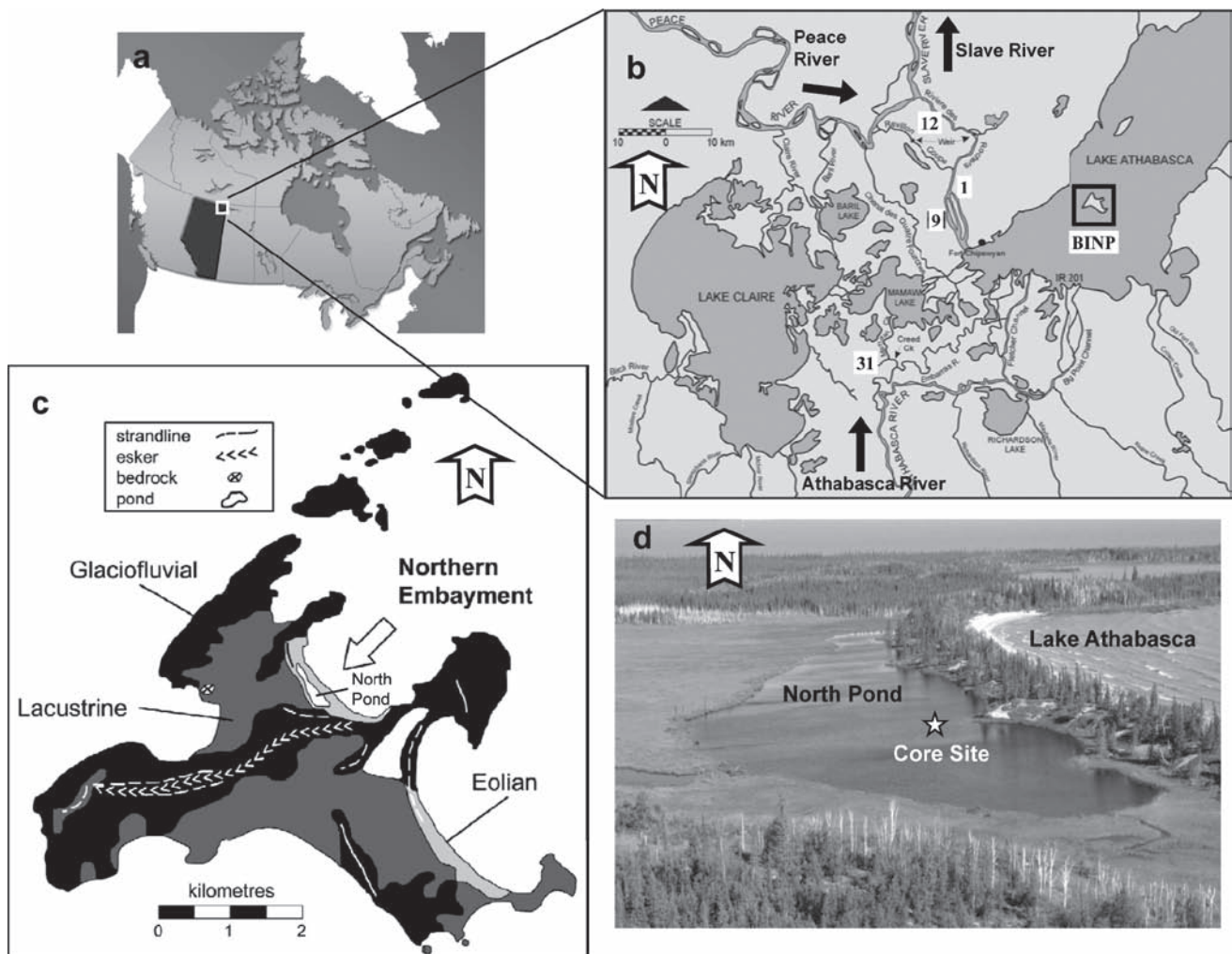


**Figure 1.** Study site and location. (a) Map of Canada with the Province of Alberta highlighted in black and the study area indicated by a square. (b) Enlarged inset of the Peace-Athabasca Delta highlighting major river courses and other cited lakes on the delta where previous research is relevant to the Bustard Island study site research presented in this paper. (c) Surficial geology of Bustard Island (modified from Bednarski, 1999). (d) Aerial photograph of the barrier-beach complex in the northern embayment on Bustard Island, including the coring site in 'North Pond'

these welded barriers have advanced landward over lagoonal deposits (Davis, 1994; Davis and Fitzgerald, 2004; Reinson, 1992).

Examination of the architecture of the northern barrier and palaeolimnological record of the adjacent lagoonal pond ('North Pond') on Bustard Island are the foci of this study. Vegetation currently covers most of this barrier, forming distinct zones of ground cover on the lakeward (crowberries) and pondward (juniper) sides of the barrier. Trees near the crest intercept mobile sediment and stabilize the barrier. The only relatively large area on the barrier that is exposed is a 2-m-high avalanching section on the pondward side that extends several metres into the lagoon. North Pond is ~2 m deep and ~7 ha in surface area, with no surface inlets or outlets. A large wetland (~24 ha) abuts the western shore of the pond.

## Methods

### Fieldwork

Sediment cores were collected from North Pond in July 2004 at a site near the base of a washover fan (15 m from the barrier, water depth 1.36 m; Figure 1c, d). A 7.5-cm diameter gravity corer (Glew, 1989) was used to collect the upper 30 cm of unconsolidated

sediment (KB2). A 10-cm diameter Russian peat corer was deployed from a floating platform to obtain a longer sequence totalling 224 cm (LC1). Russian cores were described, photographed, and wrapped in supportive PVC trays at the field site, whereas gravity cores were sectioned vertically into 0.5-cm intervals, described, and placed in individual sample bags at the field station in Fort Chipewyan before they were transported to the University of Waterloo, Canada. Samples were stored at 4°C prior to laboratory analyses.

Because several distinct sand lenses were identified in cores KB2 and LC1 (Figure 2a), additional geophysical fieldwork was conducted in July 2005 to determine the internal structure of the barrier – the likely source of the sand in the sediment cores. Two ground penetrating radar (GPR) profiles were obtained using a Sensors and Software PulseEKKO 100 system (100 and 200 MHz antennae, common-offset mode, stack of 64 measurements at each point) to examine the stratigraphic architecture of the washover fan, barrier and active beach. These included a 73 m long GPR profile recorded on land between Lake Athabasca and North Pond, and a 10 m long GPR profile extending from the base of a washover fan to the approximate lake sediment coring location was recorded from an inflatable boat. Common midpoint (CMP) surveys were also performed to determine subsurface electromagnetic wave velocity.

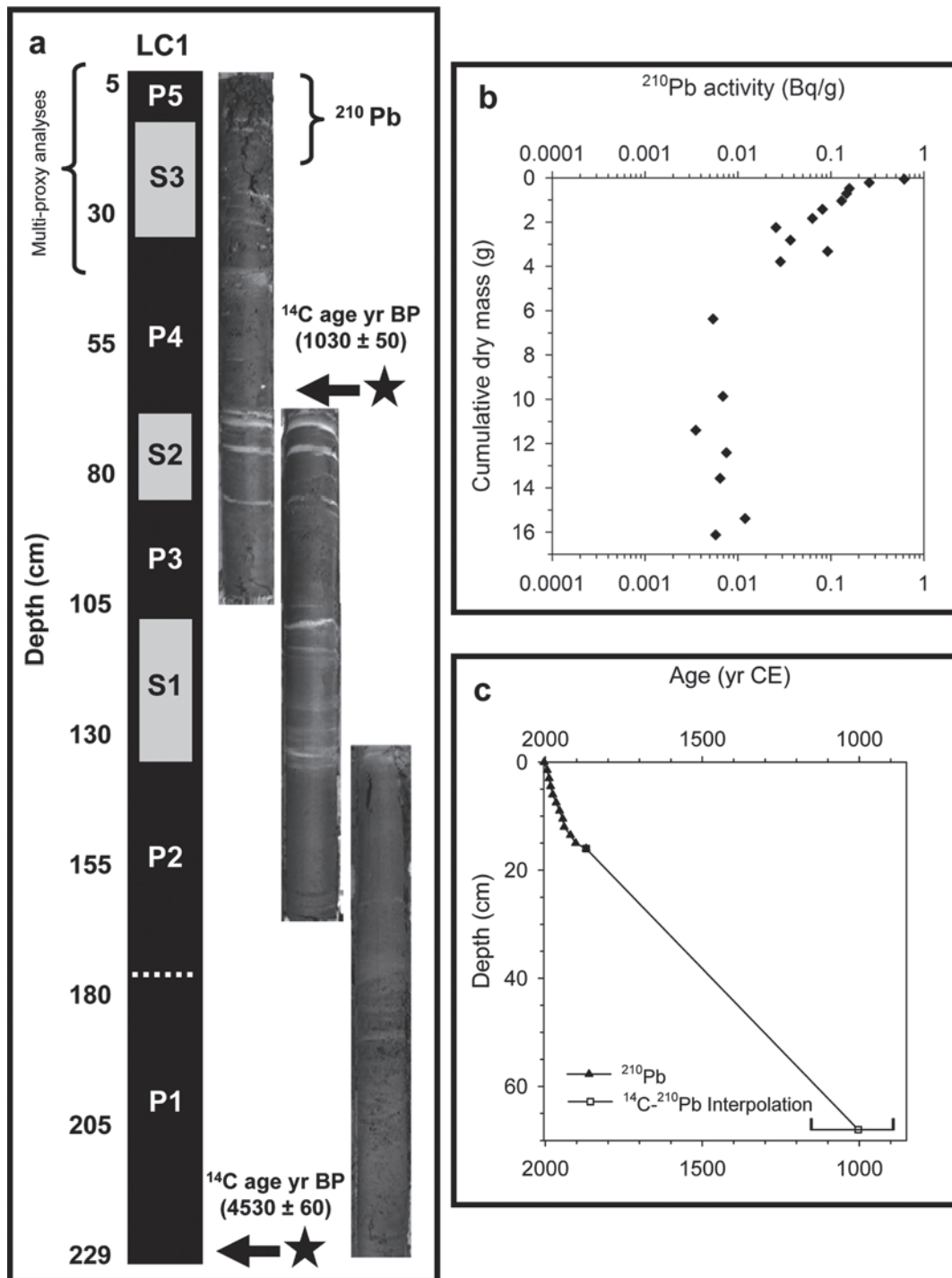


**Figure 2.** (a) Stratigraphic intervals ('P' is peat and 'S' is sand) and photographs of the North Pond long core (LC1) with two radiocarbon ages and associated depths. (b) Plot of  $^{210}\text{Pb}$  activity versus cumulative dry mass in short core (KB2). (c) Combined  $^{210}\text{Pb}$  and  $^{14}\text{C}$ - $^{210}\text{Pb}$  interpolated age–depth model for cores KB2 and LC1. A median probability radiocarbon age was used for the chronology, while the 95.4% (two sigma) calendar age ranges are shown to represent uncertainty

### Laboratory analyses

The upper 1 m of core LC1 was sectioned into 0.5-cm intervals. Moisture content, organic matter content and total carbonate content were measured on contiguous 0.5-cm samples from KB2 and every fourth sample (i.e. every 2 cm) in the upper 1 m of core LC1 by weight loss on heating (loss-on-ignition; LOI) at temperatures of 85°C, 550°C and 950°C, respectively (Heiri *et al.*, 2001). Sediment cores KB2 and LC1 were aligned using LOI results and core descriptions, which indicated the true depth for LC1 was 5–229 cm

(i.e. upper 5 cm were missing). Insufficient material precluded multiproxy analyses on all samples. Therefore, analyses were distributed between the KB2 ( $^{210}\text{Pb}$ , grain size, diatoms, macrofossils) and LC1 ( $^{14}\text{C}$ , C/N, diatoms, macrofossils) sediment cores.

The chronology for the most recent sediments (KB2, 0 to 30 cm depth) was established by the measurement of  $^{210}\text{Pb}$  activity from a known weight (0.7 to 3 g) and volume of freeze-dried sediment at 1.5 cm intervals. Samples were measured for 47 h using an ORTEC<sup>®</sup> digital gamma ray spectrometer. Calendar dates were calculated using the constant-rate-of-supply (CRS) model (Binford, 1990)

because it accounts for changes in sedimentation rates, which we expected to occur based on the visual observation of variable sand content and large variations in mineral matter content as determined from LOI analyses. Dates for sediment samples beyond the reliable age limit for  $^{210}\text{Pb}$  were estimated using linear interpolation between the oldest  $^{210}\text{Pb}$  date from KB2 and a calibrated median probability  $^{14}\text{C}$  date obtained using accelerator mass spectrometry of organic matter retrieved at 68 cm depth from core LC1 and CALIB (version 5.0) (Stuiver and Reimer, 1993). An additional  $^{14}\text{C}$  date was obtained using conventional radiocarbon analysis of organic matter from the base of core LC1. All radiocarbon analyses were performed by Beta Analytic, Inc., Miami, Florida. Radiocarbon dates were calibrated to calendar years before present by the probability distribution method using the calibration data set of Reimer *et al.* (2004).

Bulk organic carbon and nitrogen elemental content were measured at 0.5-cm intervals in core LC1. Subsamples were acid-washed with 10% HCl, rinsed with de-ionized water and freeze-dried. The fine fraction (<0.5 mm) was measured using an elemental analyser at the University of Waterloo – Environmental Isotope Laboratory.

Subsamples of sediment at 0.5-cm intervals in KB2 were sent to the Environmental Variability and Extremes Laboratory at Queen's University (Kingston ON, Canada) to determine their grain-size distributions. Pre-treatment involved removing organic matter and carbonates as well as adding a dispersant before analysis by a Beckman-Coulter LS200 laser diffraction particle-size analyser. For each sample, statistical parameters (i.e. means) were calculated by the mathematical method of moments (Krumbein and Pettijohn, 1938) and coarsest one percentile using the cumulative size distributions (Visher, 1969).

Macrofossil samples were prepared by washing 5 cm<sup>3</sup> of wet sediment samples from cores KB2 (contiguous 0.5-cm intervals) and LC1 (2 cm intervals) through a 125- $\mu\text{m}$  mesh screen with warm tap water. Material retained on the sieve was sorted in water using a binocular dissecting microscope at 8–40 $\times$  magnification and all identifiable macrofossils were enumerated. Data are presented as concentrations of macrofossils per volume of sediment. Identifications were made to the highest taxonomic resolution possible with the aid of modern reference samples as well as taxonomic keys including Bertsch (1941), Martin and Barkley (1961), Berggren (1969, 1981), Montgomery (1977) and Artjuschenko (1990).

For diatom analysis, approximately 0.5 g of wet sediment was subsampled from cores KB2 (contiguous 0.5-cm intervals) and LC1 (2-cm intervals) and digested in an equal mixture of  $\text{HNO}_3$  and  $\text{H}_2\text{SO}_4$  in a hot water bath for 6 h (Hall and Smol, 1996). The remaining solution was rinsed repeatedly to remove residual acid and microscopic slides were prepared using the optical resin Naphrax™ (refractive index: 1.73). A minimum of 500 diatom valves was counted at 1000 $\times$  magnification using a Zeiss Axioskop II plus light microscope fitted with differential interference optics and digital imaging equipment. Identification followed Krammer and Lange-Bertalot (1986–1991) and Camburn and Charles (2000).

### Ground penetrating radar processing

GPR data were processed using Sensors and Software EKKO View Deluxe software. Processing included applying a temporal (high-pass) filter to remove very low frequency signal saturation,

an automatic gain control function to compensate for signal amplitude decay and a topographic correction to reduce imaging distortions from surface elevation changes. Conversion from travel time to depth was estimated from the normal moveout analyses (Sheriff and Geldart, 1995) of CMP surveys on top of the barrier and on the beach, as well as hyperbolic matching of diffractions from subsurface objects and measured elevations from the water-table. GPR facies were defined by grouping similar GPR reflection parameters of configuration, continuity, amplitude, frequency, internal velocity and external form based on seismic stratigraphic methods of Mitchum *et al.* (1977) and radar stratigraphic methods of Neal (2004).

## Results

### North Pond sediment core description

A 229 cm long sedimentary record (adjusted after aligning the overlapping 30 cm long gravity core, KB2, and 224 cm long Russian core, LC1) collected from North Pond consists largely of peat with intervals of sand laminations (Figure 2a). A 94-cm basal sequence of peat (P1 (fibrous: 229 to 175 cm); P2 (175 to 135 cm)) is followed by three alternating intervals of sandy laminations in peat (S1 (135 to 110 cm), S2 (85 to 70 cm) and S3 (32 to 17 cm)) and dispersed sand in peat (P3 (110 to 85 cm), P4 (70 to 32 cm) and P5 (17 to 0 cm)). We focused our multiproxy analyses on the P4-S3-P5 sequence (down to 40 cm depth).

### North Pond sediment core chronology

Two samples from LC1 for radiocarbon analysis (Table 1) and 22 samples from KB2 for  $^{210}\text{Pb}$  analysis provide the chronological framework. The oldest calibrated radiocarbon age from peat (unit P1 at base of LC1, 229 cm) is between 3493 and 3025 cal. BCE (5443 and 4975 cal. BP). A median probability age using CALIB (version 5.0) (Stuiver and Reimer, 1993) is 3216 cal. BCE (5166 cal. BP). Peat typically accumulates in a low-energy back-barrier lagoonal setting and this radiocarbon date suggests the barrier beach is at least five millennia old to permit the peat to have formed landward of it. A younger radiocarbon age was obtained from 68 cm depth in LC1 (median probability age of 1003 cal. CE, 947 cal. BP) to gain age-control in the upper part of the core where multiproxy analyses were conducted.

For core KB2, the total activity of  $^{210}\text{Pb}$  decreased logarithmically with increasing cumulative dry mass and reached supported levels of 0.0286 Bq/g at 16.5 cm depth or 4.6 g/cm<sup>2</sup> cumulative dry mass (Figure 2b), corresponding to a basal CRS-modeled  $^{210}\text{Pb}$  date of 1861. Linear interpolation between this date and the younger of the two  $^{14}\text{C}$  dates was used to establish a sediment chronology between 16.5 cm and 68 cm depth (Figure 2c).

### North Pond sediment core multiproxy data (1500 CE to present)

Geochemical, physical and biological proxy data obtained from the North Pond KB2 and LC1 sediment cores are assembled in Figure 3 and are shown in relation to the three-phase hydroecological history of pond PAD 9 during the past 400 years, as captured by key diatom profiles (Sinnatamby *et al.*, 2010). The PAD 9 record and historical maps provide evidence of an expansion of Lake Athabasca into the PAD during the LIA (~1600–1875),

**Table 1.** Radiocarbon data for lake sediment core from Bustard Island North Pond

Lab. number	Material	Sediment core depth	Reported age	Calibrated two sigma (95.4%) age ranges	Relative area under distribution	Median probability
Beta-223382	Organic sediment	68 cm	1030 ± 50 <sup>14</sup> C yr BP	892–1052 and 1080–1153 cal. CE	0.85 0.15	1003 cal. CE
Beta-205361	Peat	229 cm	4530 ± 60 <sup>14</sup> C yr BP	3493–3468 and 3374–3079 and 3070–3025 cal. BCE	0.02 0.93 0.05	3216 cal. BCE

Radiocarbon dates were calibrated to calendar years before present using the program CALIB (version 5.0) (Stuiver and Reimer, 1993) with the calibration data set of Reimer et al. (2004).

followed by a transitional period characterized by flow-through lake conditions in PAD 9 (~1875–1925), and by a period of closed-drainage hydrological conditions (~1925 to present).

Carbon to nitrogen (C/N) weight ratios from North Pond core LC1 range from 13.1 to 16.4 (Figure 3). C/N ratios decline from 16.4 to 13.6 in the dispersed sand in peat interval P4 and then remain low throughout the sandy laminations in peat interval S3. The change in C/N values at the P4–S3 boundary at North Pond coincides with the start of a highstand of Lake Athabasca recorded at PAD 9. No obvious change in the C/N ratio occurs between S3 and P5. C/N values increase after 1935, attaining a ratio of ~15 in the most recent sediments.

The lithology of sediments of North Pond core KB2 ranges from clay to sand, with sand dominating most of the core (85 to ~99 cumulative percent) (Figure 3). Mean grain size ranges from fine sand to coarse silt, while the coarsest one percentile (C1%) ranges from very coarse sand to medium sand. In the sandy laminations in peat interval S3, sand content is high (mean ~93%), mean grain size is mainly fine sand and C1% oscillates between very coarse sand and medium sand. In the lower part of P5, sand content decreases to as low as 73% and fine-grained sediment (silt and clay) content increases, mean grain size decreases to very fine sand and C1% becomes more consistently finer-grained (medium sand) compared with the episodic variations below. These trend changes occur around the mid 1800s and are of similar age to the transition at pond PAD 9 from inundation under the LIA highstand on Lake Athabasca to a flow-through lake. At North Pond, the upper part of zone P5 displays consistent trends of increasing silt and clay content (and declining sand content), decreasing mean grain size to coarse silt and decreasing C1% to medium sand.

Relative abundance of epiphytic diatom taxa (mainly from the genera *Diploneis*, *Gomphonema*, and *Stauroneis*) was high between c. 1500 and 1750 CE when macrofossils from emergent and submergent macrophytes were most abundant, but abundance of all these taxa declined thereafter (Figure 3). Since ~1900, relative abundance of acidophilic diatom taxa (*Eunotia* spp., *Pinnularia pluvianiformis*) increased, while epiphytic taxa declined to very low values. This latter change coincides with several-fold increases in the abundance of macrofossils from *Sphagnum* mosses and terrestrial plants (*Betula*, *Ericacea*; Figure 3).

### Barrier morphology and stratigraphy

A composite 83 m long GPR profile extending from near the North Pond coring site, across the washover fan and barrier, to the modern Lake Athabasca shoreline delineates architectural features within the barrier (Figure 4A). Five sedimentary facies (I–V) were identified from the GPR profiles (Figure 4B). The

maximum depth of penetration using both the 100 and 200 MHz GPR antennae (11.75 m depth at the barrier crest) corresponds to the base of the washover fan and top of the North Pond sediment core. A common limiting depth for two different GPR frequencies suggests the underlying material properties in facies I are finer-grained than the overlying material properties in facies II–V.

Four facies comprise the barrier, all likely composed of similar material but with differing internal structures (facies II–V in Figure 4). Observed surface sediments across the barrier and sediment within a 1 m high exposure on the lakeward side of the barrier indicate facies III to V consist largely of sand. The electromagnetic wave velocities obtained from the analyses of the CMP surveys collected from the top of the barrier (0.14 m/ns) and active beach (0.06 m/ns) are consistent with values for unsaturated and saturated sand, respectively (cf. Annan, 2003). Facies II, which extends almost 5 m below the relatively horizontal water-table, spans the entire length of the 83 m GPR profile with internal reflections forming sigmoidal surfaces that build laterally toward North Pond. The base of facies II is defined by sigmoidal surfaces asymptotically approaching a common horizontal to subhorizontal surface that defines the maximum depth of penetration. The top of facies II coincides with a large change in amplitude that is associated with the water-table. Facies III spans up to about 60 m in length and is approximately 4 m thick under the barrier crest. Although few sigmoidal surfaces extend up into facies III from facies II, facies III predominantly consists of several parallel to subparallel reflections, several of which extend horizontally across the entire length of the profile but are elsewhere discontinuous. Facies IV and V extend over approximately 35 m and are about 3 m thick under the barrier crest. Facies IV has a fairly chaotic arrangement of reflecting surfaces with no apparent stratification. Scattering from near-surface objects such as roots may contribute to this pattern. Facies V forms a wedge on the pondward side of facies IV and contains several sigmoidal surfaces that dip towards North Pond.

### Discussion

Water levels in North Pond should closely track changes in the water plane of Lake Athabasca, as reported elsewhere for many lakes, ponds and wetlands that occur behind permeable unconsolidated coastal barriers (Peterson et al., 2007). This is supported by field observations, which include similar surveyed elevations of North Pond and Lake Athabasca, and the nature of sediments exposed on the surface and GPR velocities in the subsurface indicating the barrier is composed of coarse-grained sediment. Thus, former highstands of Lake Athabasca should also have occurred in North Pond. No washover sediments occur on top of the 6.6

**PAD 9**

**Bustard Island North Pond**

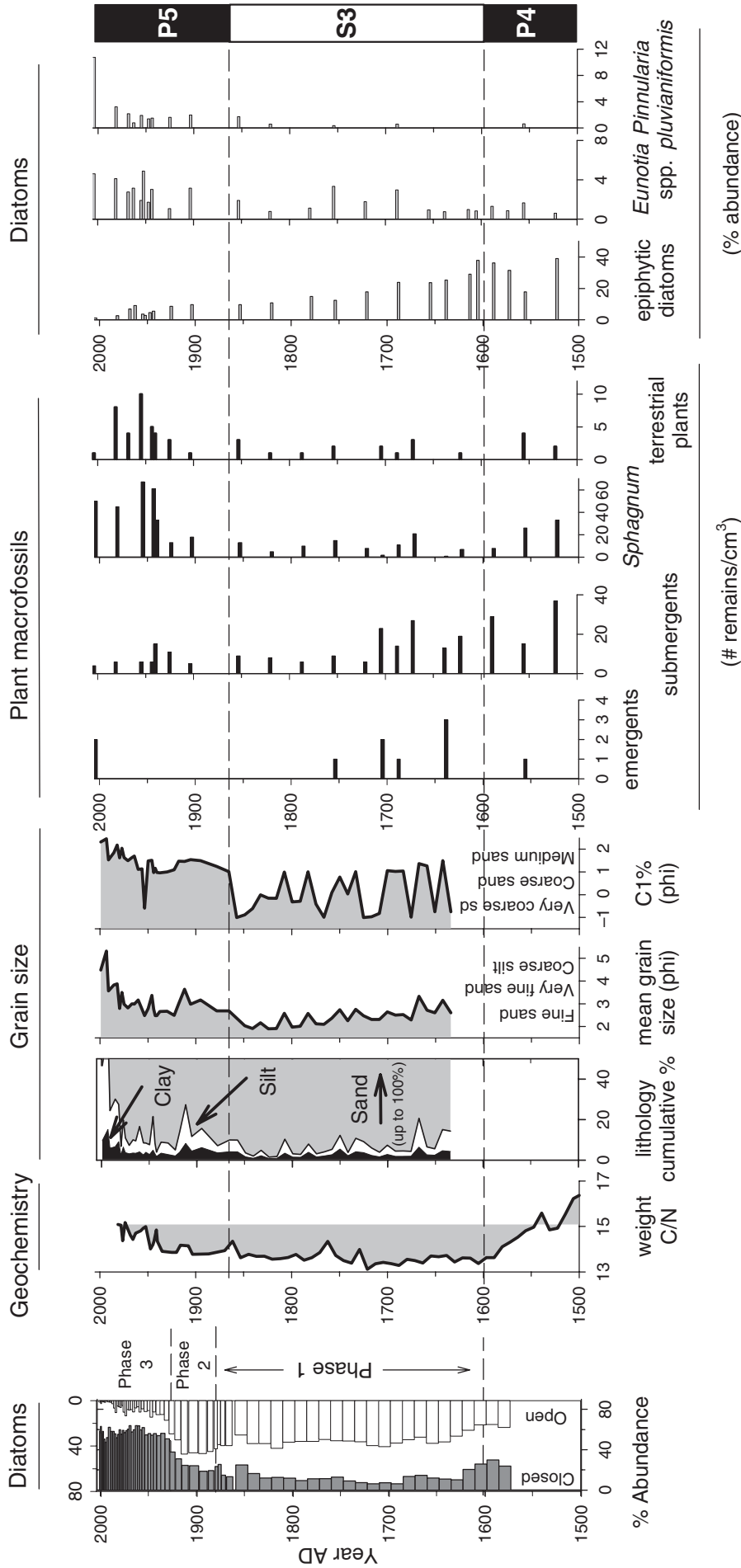


**Figure 3.** Stratigraphic plot comparing summary of key palaeolimnological indicators from PAD 9 and Bustard Island North Pond. PAD 9 diatom profiles indicate the sum of closed-drainage indicator taxa (grey) and *Staurirella pinnata*, an abundant open-drainage indicator taxa (open); hydrological phases from pond PAD 9 in the Peace-Athabasca Delta are also shown (from Sinnatambay et al., 2010)

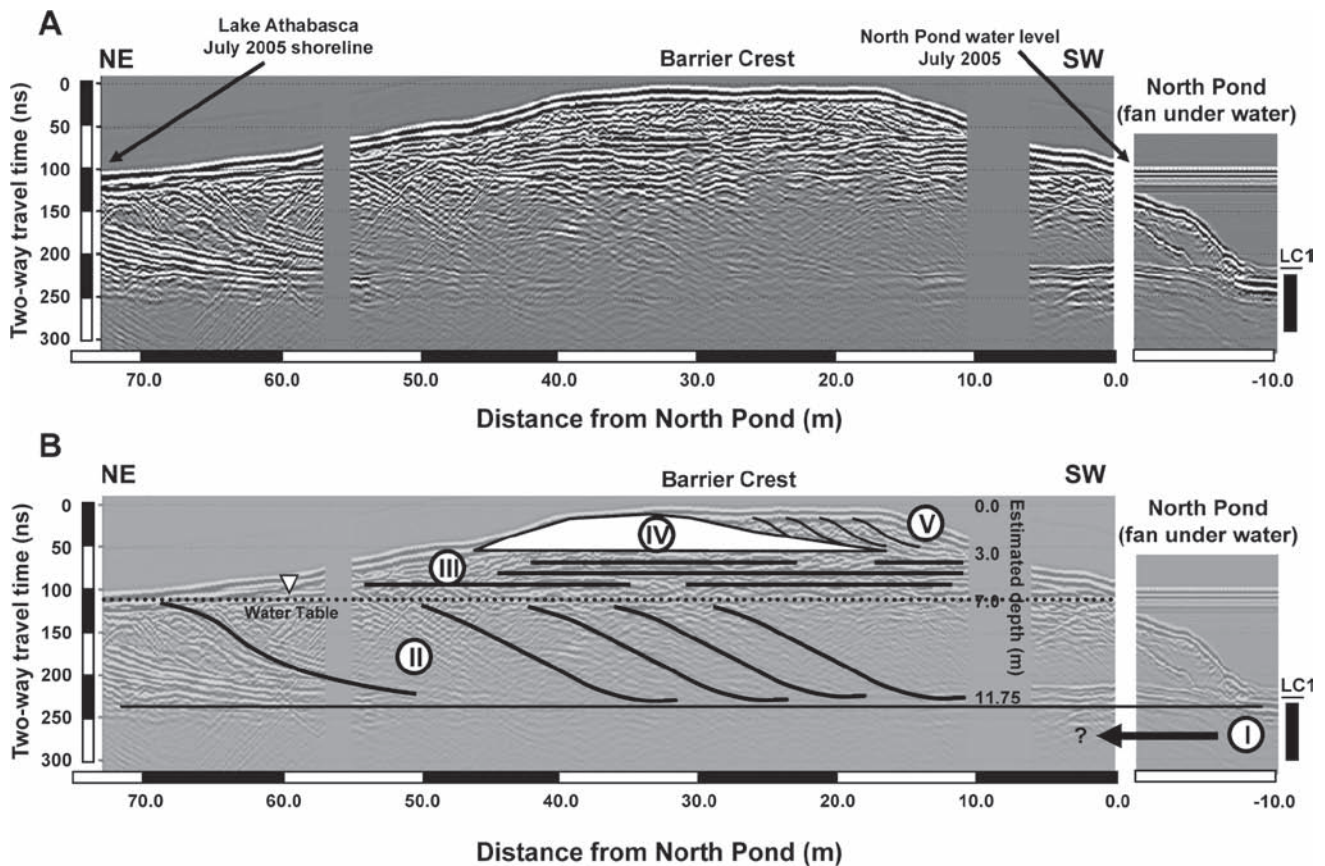


**Figure 4.** Ground-penetrating radar (GPR) profiles (raw (A) and interpreted (B)) across the Bustard Island barrier from Lake Athabasca to the North Pond. Five GPR facies (I–V) are identified

to 6.9 m high barrier, indicating that the most recent highstand of Lake Athabasca was less than the current height of the barrier. As discussed below, insight into the evolution of the barrier stratigraphy constrains the probable elevation of Lake Athabasca during the LIA highstand, which also explains the deposition of the washover deposits (i.e. sand laminations) in the North Pond S3 stratigraphic interval (Figure 3).

#### *Evidence from North Pond sediments of a Lake Athabasca highstand during the 'Little Ice Age'*

Several lines of evidence from multiproxy analyses of the North Pond sediment record (Figure 3) provide support for a Lake Athabasca highstand during the LIA (~1600–1900 CE), consistent with evidence obtained from the record at PAD 9 (Sinnatamby *et al.*, 2010; Wolfe *et al.*, 2008). (1) We interpret the carbon to nitrogen (C/N) weight ratio in North Pond sediments to be reflective of changes in the delivery of terrestrial organic matter relative to aquatic organic matter (cf. Meyers and Teranes, 2001), as the pond expanded and contracted in response to changes in Lake Athabasca levels. Consistently low C/N ratios during the LIA can be explained readily by persistently high water levels in North Pond because this would have reduced the supply of terrestrial material reaching the coring site. (2) Coarse mean grain size of the inorganic fraction at this time indicates high energy, and fluctuating C1% values reflect a variable traction load that is consistent with deposition by overwash processes. (3) An initial increase in abundance of submerged aquatic macrophyte remains is consistent with increasing water-column depth for these plant communities

and which provide additional habitat for proliferation of epiphytic diatoms during the onset of the LIA.

The stratigraphic patterns before and after the LIA contrast with those during the LIA (Figure 3). For example, elevated C/N ratios during the 1500s and in the late twentieth century are likely due to low water levels at North Pond because contraction of the lake would lead to an increase in delivery of terrestrial organic matter to the coring location. The inorganic fraction in post-LIA sediments is generally dispersed (i.e. few laminations) and finer grained with a less variable and finer C1%, which is more typical of aeolian- than washover-derived sediments. As lake levels declined after the LIA, elevated abundance of macrofossils from *Sphagnum* moss and terrestrial plants, as well as increases in the acidophilous moss epiphyte diatoms *Eunotia* spp. and *Pinnularia pluvianiformis*, also suggest encroachment of wetland and terrestrial plant communities into North Pond.

#### *Estimation of Lake Athabasca water level during the 'Little Ice Age' from barrier stratigraphy*

Analysis of the composite 83 m long GPR profile extending from near the North Pond coring site, across the washover fan and barrier, to the modern Lake Athabasca shoreline defines five different sedimentary facies (Figure 4) that are typical of transgressive barriers (Kraft, 1971; Moller and Anthony, 2003; Schwartz, 1975, 1982; Smith *et al.*, 2003). The abrupt base of GPR penetration corresponds to the top of the North Pond sediment record (consisting of predominantly peat) and indicates that the barrier is likely over-riding fine-grained lagoonal deposits that do not

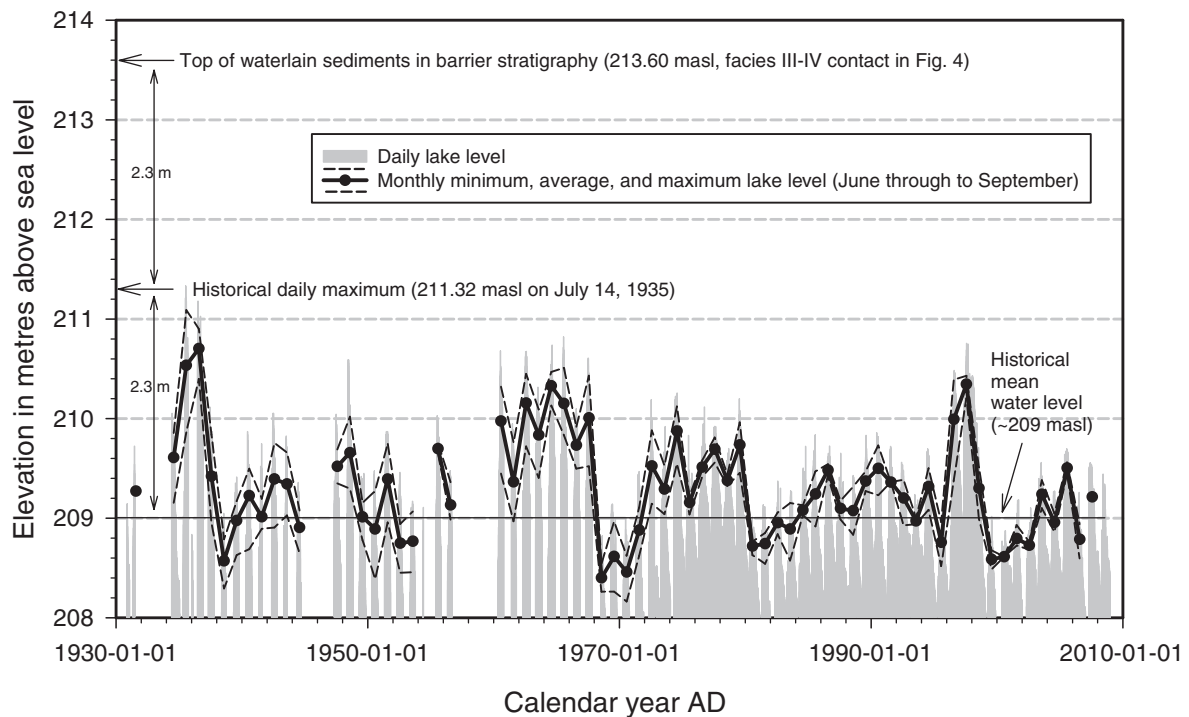


**Figure 5.** Fort Chipewyan daily and monthly (open-water months of June to September) gauged water-level data for Lake Athabasca (1930 to 2008). Data retrieved from the National HYDAT database (Environment Canada, 2009)

return a GPR signature (facies I in Figure 4). GPR-imaged horizontal stratification (facies III) over foreset stratification (facies II) effectively captures the superposition of proximal (topset) over distal (foreset) fan sediment as the barrier advanced pondward. The horizontal stratification is related to upper plane bed (high energy) conditions under which large quantities of sediment are transported by sheet flow, whereas the foreset stratification is related to slipface migration of an advancing front where sediments terminate in standing water. We interpret the most recent overwash events in the North Pond sediment record (sand laminations in S3; Figure 3) to represent the distal edge of the delta foresets and, thus, they correlate temporally with the uppermost waterlain topset beds. Chaotic GPR reflections, typical of soil development in dune sediment, form the barrier crest (facies IV). Given that the most recent washover deposits were formed during the LIA, this would then imply that the contact between the waterlain topsets (facies III) and windblown sediments (facies IV) is the elevation (213.60 m a.s.l.) of the water plane when washover sediments were transported into North Pond. Hence, this also provides a conservative estimate of the maximum elevation of Lake Athabasca during the LIA that can be refined further using the historical water-level record of Lake Athabasca.

The Lake Athabasca water-level gauge record at Fort Chipewyan (Environment Canada, 2009) (Figure 5), which has been operational since 1930 and is closest to Bustard Island, indicates annual maximum water levels generally occur in July (average ~209 m a.s.l.). The historical maximum water level of 211.32 m a.s.l. occurred on 14 July 1935, which was likely storm-related. Notably, the elevation of the contact between the uppermost waterlain horizontal stratification (facies III in Figure 4) and the dune sand (facies IV; Figure 4) that caps the barrier on Bustard Island (213.60 m a.s.l.) is about twice the difference between the average Lake Athabasca level (209 m a.s.l.) and the maximum daily water level (211.32 m a.s.l.) recorded at the Fort Chipewyan

gauge. In other words, our analysis indicates that during the LIA, Lake Athabasca water level was, at times, ~4.6 m higher than the historical average to produce the washover deposits in North Pond. Assuming that a similar difference between average and maximum water level in the historical gauge record persisted during the LIA highstand, we estimate that the *average* water level of Lake Athabasca during the LIA was ~211.3 m a.s.l., i.e. 2.3 m above the *historical average* water level and equal to the *historical daily maximum*.

#### *Submergence of the lowland interior of the Peace-Athabasca Delta during the 'Little Ice Age'*

How would the Peace-Athabasca Delta (PAD) have appeared during the LIA, assuming a 2.3-m highstand in the average level of Lake Athabasca? A digital elevation model (Peters *et al.*, 2006; Pietroniro *et al.*, 1996, 1999) and extrapolation of a 211 m a.s.l. high-water plane shows that almost the entire lowland central corridor of the PAD (Figure 6), including the large lakes Claire and Mamawi, would have been confluent, forming one large, shallow water body. This is consistent with palaeolimnological evidence from basins PAD 1, 9 and 31 situated near the margins of this postulated Lake Athabasca embayment, which shows open-drainage conditions during the LIA that are markedly different from their current states (Figure 7). To the north, diatom assemblages in sediments from PAD 9 identify turbid open-drainage hydrological conditions that promote dominance by small benthic Fragilariaceae (Sinnatamby *et al.*, 2010; Wolfe *et al.*, 2008). Additionally, high values of  $\delta^{13}\text{C}$  in sediments deposited during this interval at nearby PAD 1 are consistent with inundation under the LIA highstand of Lake Athabasca, because modern  $\delta^{13}\text{C}$  measurements of phytoplankton are higher in open-drainage systems than in closed-drainage systems in the spring (Light, 2010; Lyons, MSc Thesis, in preparation). A diatom record from pond PAD 12 along the Rivière

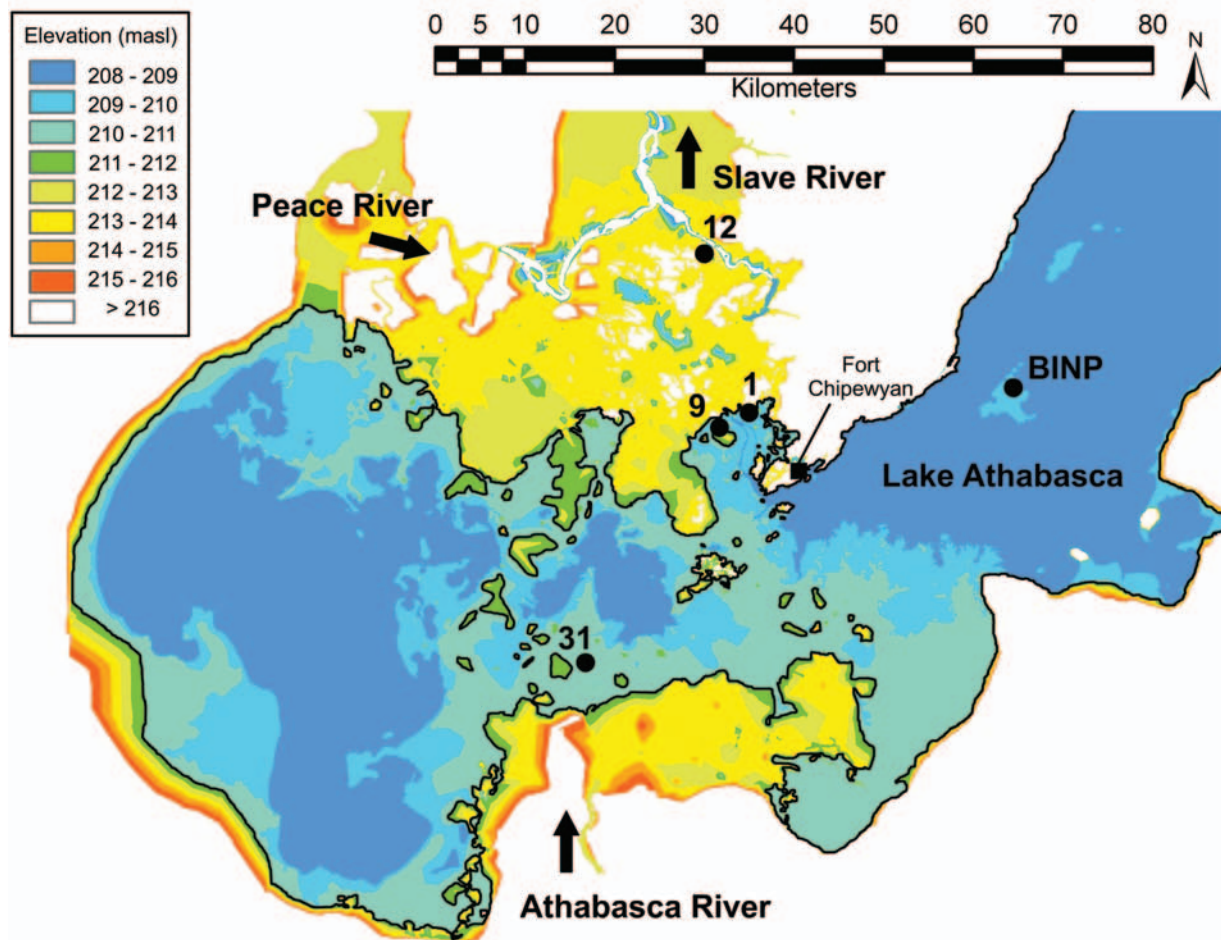


**Figure 6.** Modified digital elevation model of Peters *et al.* (2006) with lakes from which other palaeolimnological records have been obtained indicated by numbers (PAD 1, 9, 12, 31). Bold contour line identifies the 211 m a.s.l. water plane during the 'Little Ice Age'

des Rochers identified areas that were outside the main embayment that also contain evidence of open-drainage conditions resulting from elevated discharge from Lake Athabasca (Wolfe *et al.*, 2008). To the south and within the embayment, PAD 31 also shows a large increase in diatom taxa associated with open-drainage conditions as a result of inundation by Lake Athabasca during the LIA (Figure 7). Peak abundance of open-drainage indicator diatom taxa occurred ~1600–1770, suggesting that highest Lake Athabasca water levels occurred at this time. Interestingly, many bedrock exposures to the northeast of Mamawi Lake show high water marks ~2 m above present-day water level – a likely remnant of a very different landscape of the LIA that occurred little more than 100 years ago.

## Conclusion

Interpretation of multiproxy palaeolimnological results and GPR stratigraphy of a transgressive barrier-beach complex in Lake Athabasca supports quantitative reconstruction of lake levels during the 'Little Ice Age' (1600–1900 CE). Our analysis indicates average water levels were 2.3 m higher than the historical average from 1930–present gauge records and that extreme storm events would likely have raised lake level by an additional 2.3 m. These findings indicate that the present-day wetland-dominated interior of the adjacent Peace-Athabasca Delta was entirely submerged during the LIA, consistent with open-drainage hydrological conditions reconstructed from several lakes along the margin of a

shallow western embayment of Lake Athabasca. This would have created one confluent water body, connecting Lake Athabasca to Richardson Lake, Mamawi Lake and Lake Claire, or about three times the area currently covered by water in the PAD during average historical conditions. The approach demonstrated here, incorporating both GPR-based stratigraphic analysis of a beach-barrier complex and palaeolimnological analyses of lagoonal sediments, provides new opportunities for developing additional quantitative water-level reconstructions for Lake Athabasca as well as for other large lakes.

The Bustard Island barrier is currently in a quiescent stage fostered by a combination of low average water levels in Lake Athabasca, vegetation growth since the mid to late 1800s (Bailey, 2008) and the development of a thick dune cap (~3 m) on top of the barrier, which has helped to stabilize it. This is in marked contrast to the active stage that occurred during the LIA when the barrier was advancing towards North Pond as sediment was eroded on the lakeward margin and added to the pondward margin. Notably, previous cycles of instability and stability are apparent in the North Pond stratigraphy, captured by intervals (in deeper sediments than those analysed here) of peat deposition with sand laminations and peat with dispersed sand (Figure 2a), respectively. Linear extrapolation to the basal radiocarbon age (5290 cal. BP) suggests these cycles may vary on timescales of about a millennium and will be the subject of further study.

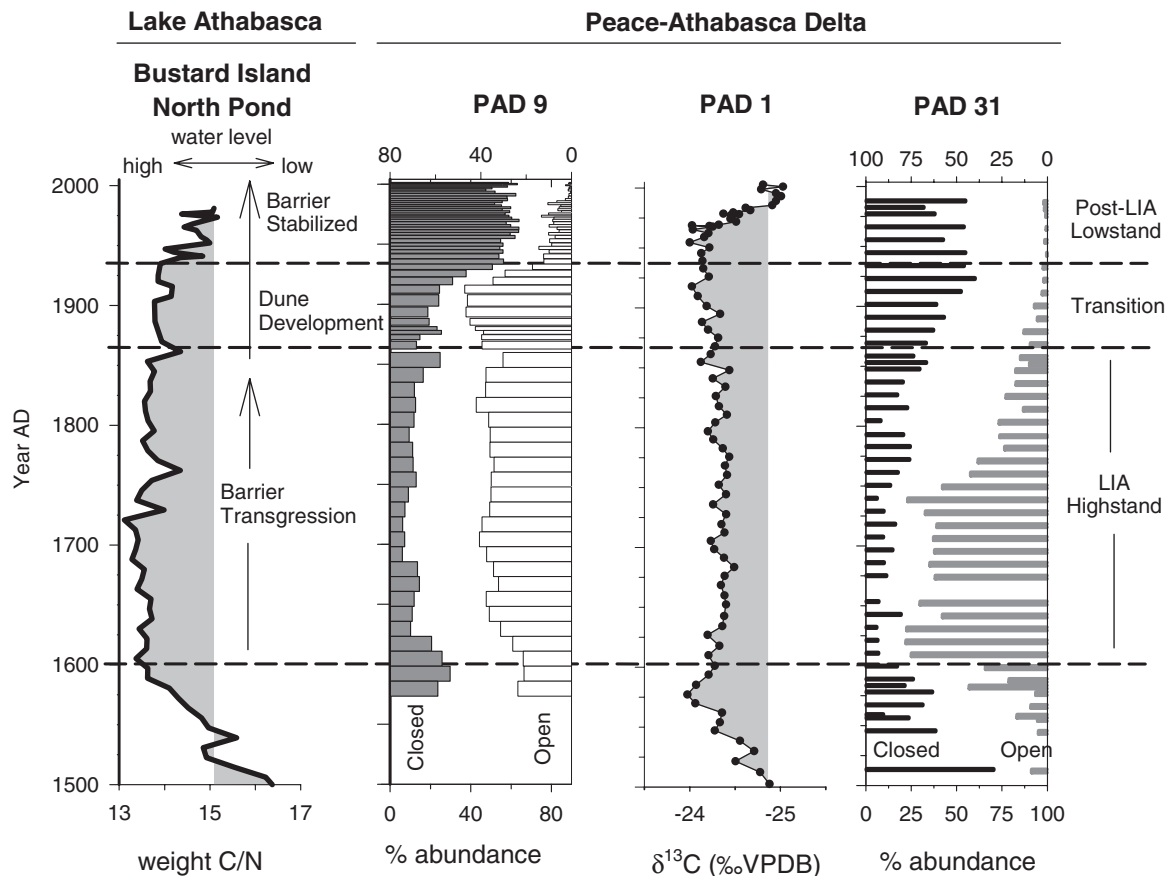


**Figure 7.** Palaeolimnological records, including the C/N ratio profile from Bustard Island North Pond (this study), the PAD 9 summary diatom record (Sinnatamby *et al.*, 2010), the PAD 1 organic carbon isotope ( $\delta^{13}\text{C}_{\text{org}}$ ) record (Light, 2010) and PAD 31 summary diatom record (Wiklund, PhD thesis, in progress)

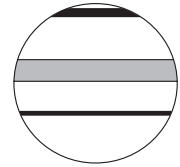
## Acknowledgements

We thank staff of Wood Buffalo National Park for logistical support. Field assistance was provided by Jolene Boucher, Suzanne Jarvis, Niloshini Sinnatamby, and Yi Yi; laboratory assistance was provided by Paige Harms. Funding was provided by the NSERC Northern Research Chair, Discovery, and Collaborative and Research Development grant programs, British Columbia Hydro and Power Authority, Government of Ontario Premier's Research Excellence Awards, the Polar Continental Shelf Project and the Northern Scientific Training Program of Indian and Northern Affairs Canada.

## References

- Annan AP (2003) *Ground Penetrating Radar – Principles, Procedures and Applications*. Sensors and Software.
- Artjuschenko Z (1990) *Organographia Illustrata Plantarum Vascularium*. Institutum Botanicum Nomina V Kamrovii (in Russian with Latin).
- Baedke SJ, Thompson TA (2000) A 4,700-year record of lake level and isostasy for Lake Michigan. *Journal of Great Lakes Research* 26: 416–426.
- Bailey JN-L (2008) Reconstruction of paleoclimate time-series in the Peace-Athabasca Delta, northern Alberta, from stable isotopes in tree-rings. MSc Thesis, Earth and Environmental Sciences, University of Waterloo.
- Bednarski JM (1999) *Quaternary Geology of Northeastern Alberta*. Geological Survey of Canada Bulletin 535.
- Berggren G (1969) *Atlas of Seeds and Small Fruits of Northwest-European Plant Species: Part 2. Cyperaceae*. Swedish Natural Science Research Council.
- Berggren G (1981) *Atlas of Seeds and Small Fruits of Northwest-European Plant Species: Part 3. Salicaceae–Cruciferae*. Swedish Natural Science Research Council.
- Bertsch K (1941) *Handbuecher der praktischen Vorgeschichtsforschung, Band 1: Fruchte und Samen*. Stuttgart: Verlag Ferdinand Enke.
- Binford MW (1990) Calculation and uncertainty analysis of 210Pb dates for PIRLA project lake sediment cores. *Journal of Paleolimnology* 3: 253–267.
- Camburn KE, Charles DF (2000) *Diatoms of Low Alkalinity Lakes in Northeastern United States*. Academy of Natural Sciences Special Publication 18.
- Davis RA Jr (1994) Barrier island systems – a geologic overview. In: Davis RA Jr (ed.) *Geology of Holocene Barrier Island Systems*. Springer-Verlag, 1–46.
- Davis RA Jr, Fitzgerald DM (2004) *Beaches and Coasts*. Blackwell Science.
- Environment Canada (2009) Archived hydrometric data, National HYDAT database. Available at <http://www.wsc.ec.gc.ca/hydat/H2O/>
- Glew JR (1989) A new trigger mechanism for sediment samplers. *Journal of Paleolimnology* 2: 241–243.
- Hall RI, Smol JP (1996) Paleolimnological assessment of long-term water-quality changes in south-central Ontario lakes affected by cottage development and acidification. *Canadian Journal of Fisheries and Aquatic Sciences* 53: 1–17.

- Heiri O, Lotter AF and Lemcke G (2001) Loss on ignition as a method for estimating organic and carbonate content in sediments: Reproducibility and comparability of results. *Journal of Paleolimnology* 25: 101–110.
- Johnston JW, Baedke SJ, Booth RK, Thompson TA and Wilcox DA (2004) Late Holocene lake-level variation in southeastern Lake Superior: Tahquamenon Bay, Michigan. *Journal of Great Lakes Research* 30: 1–19.
- Johnston JW, Thompson TA, Wilcox DA and Baedke SJ (2007) Geomorphic and sedimentologic evidence for the separation of Lake Superior from Lake Michigan and Huron. *Journal of Paleolimnology* 37: 349–364.
- Kraft JC (1971) Sedimentary facies patterns and geologic history of a Holocene marine transgression. *Geological Society of American Bulletin* 82: 2131–2158.
- Krammer K, Lange-Bertalot H (1986–1991) *Susswasserflora von Mitteleuropa, Band 2*. Gustav Fischer Verlag.
- Krumbein WC, Pettijohn FJ (1938) *Manual of Sedimentary Petrography*. Appleton-Century.
- Light C (2010) Identifying potential carbon flux responses to shifting hydroecological and climatic regimes in the Peace-Athabasca Delta. MSc Thesis, Geography and Environmental Studies, Wilfrid Laurier University.
- Martin AC, Barkley WD (1961) *Seed Identification Manual*. University of California Press.
- Meyers PA, Teranes JL (2001) Sediment organic matter. In: Last WM, Smol JP (eds) *Tracking Environmental Change Using Lake Sediments, Physical and Geochemical Methods, Vol 2*. Dordrecht: Kluwer, 239–269.
- Mitchum RM, Vail PR and Sangree JB (1977) Seismic stratigraphy and global changes of sea level, Part 6: Stratigraphic interpretation of seismic reflection patterns in depositional sequences. In: Payton CE (ed.) *Seismic stratigraphy – applications to hydrocarbon exploration. American Association of Petroleum Geologists Memoir* 26, 117–133.
- Moller I, Anthony D (2003) A GPR study of sedimentary structures within a transgressive coastal barrier along the Danish North Sea coast. In: Bristow CS, Jol HM (eds) *Ground Penetrating Radar in Sediments*. The Geological Society of London Special Publication 211: 55–65.
- Montgomery FH (1977) *Seed and Fruit Plants of Eastern Canada and Northeastern United States*. University of Toronto Press.
- Neal A (2004) Ground-penetrating radar and its use in sedimentology: Principles, problems and progress. *Earth-Science Reviews* 66: 261–330.
- Peters DL, Prowse TD, Pietroniro A and Leconte R (2006) Flood hydrology of the Peace-Athabasca Delta, northern Canada. *Hydrological Processes* 20: 4073–4096.
- Peterson CD, Jol HM, Percy D and Nielsen EL (2007) Groundwater surface trends from ground penetrating radar (GPR) profiles taken across Late Holocene barriers and beach plains of the Columbia River littoral system, Pacific Northwest Coast, USA. In: Baker GS, Jol HM (eds) *Stratigraphic Analysis Using GPR*. The Geological Society of America Special Paper 432, 59–76.
- Pietroniro A, Prowse TD and Jordan S (1996) *Generating a Spatial and Temporal Database for the Peace-Athabasca Delta Study Region*. Peace-Athabasca Delta Technical Studies, Task D.1 – Topographic Database.
- Pietroniro A, Toyra J and Best K (1999) *Mapping the 1996 Peace-Athabasca Delta Floods*. National Water Research Institute 98–262, Environment Canada.
- Polderman NJ, Pryor SC (2004) Linking synoptic-scale climate phenomena to lake-level variability in the Lake Michigan-Huron basin. *Journal of Great Lakes Research* 30: 419–434.
- Reimer PJ, Baillie MGL, Bard E, Bayliss A, Beck JW, Bertrand CJH et al. (2004) IntCal04 terrestrial radiocarbon age calibration, 26–0 ka BP. *Radiocarbon* 46: 1029–1058.
- Reinson GE (1992) Transgressive barrier island and estuarine systems. In: Walker RG, James NP (eds) *Facies Models, Response to Sea Level Changes*. Geological Association of Canada, 179–194.
- Schwartz RK (1975) *Nature and Genesis of Some Storm Washover Deposits*. Coastal Engineering Research Center, Technical Memorandum 61.
- Schwartz RK (1982) Bedform and stratification characteristics of some modern smallscale washover sand bodies. *Sedimentology* 29: 835–849.
- Sheriff RE, Geldart LP (1995) *Exploration Seismology*. Cambridge University Press.
- Sinnatamby RN, Yi Y, Sokal MA, Clogg-Wright KP, Asada T, Vardy SR et al. (2010) Historical and paleolimnological evidence for expansion of Lake Athabasca (Canada) during the Little Ice Age. *Journal of Paleolimnology* doi: 10.1007/s10933-009-9361-4.
- Smith DG, Simpson CJ, Jol HM, Meyers RA and Currey DR (2003) GPR stratigraphy used to infer transgressive deposition of spits and a barrier, Lake Bonneville, Stockton, Utah, USA. In: Bristow CS, Jol HM (eds) *Ground Penetrating Radar in Sediments*. The Geological Society of London Special Publication 211, 79–86.
- Stuiver M, Reimer PJ (1993) Extended <sup>14</sup>C database and revised CALIB radiocarbon calibration program. *Radiocarbon* 35: 215–230.
- Thompson TA, Baedke SJ (1997) Strandplain evidence for late Holocene lake-level variations in Lake Michigan. *GSA Bulletin* 109: 666–682.
- Visher GS (1969) Grain size distributions and depositional processes. *Journal of Sedimentary Petrology* 39: 1074–1106.
- Wolfe BB, Hall RI, Edwards TWD, Jarvis SR, Sinnatamby RN, Yi Y et al. (2008) Climate-driven shifts in quantity and seasonality of river discharge over the past 1000 years from the hydrographic apex of North America. *Geophysical Research Letters* 35: L24402 doi:10.1029/2008GL036125.



---

## Erratum

The Holocene  
20(5) 812  
© The Author(s) 2010  
Reprints and permission:  
[sagepub.co.uk/journalsPermissions.nav](http://sagepub.co.uk/journalsPermissions.nav)  
DOI: 10.1177/0959683610374164  
<http://hol.sagepub.com>  


John W. Johnston, Dörte Köster, Brent B. Wolfe, Roland I. Hall, Thomas W.D. Edwards, Anthony L. Endres, Margaret E. Martin, Johan A. Wiklund and Caleb Light (2010): Quantifying Lake Athabasca (Canada) water level during the 'Little Ice Age' highstand from palaeolimnological and geophysical analyses of a transgressive barrier-beach complex. (Original DOI: 10.1177/0959683610362816).

The following errors occurred during editorial handling of this article:

p. 1, last sentence of Abstract:

Extrapolation of this high-water plane into the adjacent Peace-Athabasca Delta indicates that 70% of the modern landscape was frequently and perennially flooded until very recently, consistent with palaeolimnological evidence from several lakes in the delta.

This sentence should read:

Extrapolation of this high-water plane into the adjacent Peace-Athabasca Delta indicates that 70% of the modern landscape was frequently or perennially flooded until very recently, consistent with palaeolimnological evidence from several lakes in the delta.

p. 9, third sentence of Conclusion:

These findings indicate that the present-day wetland-dominated interior of the adjacent Peace-Athabasca Delta was entirely submerged during the LIA, consistent with open-drainage hydrological conditions reconstructed from several lakes along the margin of a shallow western embayment of Lake Athabasca.

This sentence should read:

These findings indicate that the present-day wetland-dominated interior of the adjacent Peace-Athabasca Delta was often almost entirely submerged during the LIA, consistent with open-drainage hydrological conditions reconstructed from several lakes along the margin of a shallow western embayment of Lake Athabasca.